

PlainMamba: Improving Non-Hierarchical Mamba in Visual Recognition

Chenhongyi Yang^{*1}, Zehui Chen^{*2}, Miguel Espinosa^{*1}, Linus Ericsson¹, Zhenyu Wang³, Jiaming Liu³, and Elliot J. Crowley¹

¹ School of Engineering, University of Edinburgh

² University of Science and Technology of China

³ Peking University

Abstract. We present PlainMamba: a simple non-hierarchical state space model (SSM) designed for general visual recognition. The recent Mamba model has shown how SSMs can be highly competitive with other architectures on sequential data and initial attempts have been made to apply it to images. In this paper, we further adapt the selective scanning process of Mamba to the visual domain, enhancing its ability to learn features from two-dimensional images by (i) a *continuous 2D scanning* process that improves spatial continuity by ensuring adjacency of tokens in the scanning sequence, and (ii) *direction-aware updating* which enables the model to discern the spatial relations of tokens by encoding directional information. Our architecture is designed to be easy to use and easy to scale, formed by stacking identical PlainMamba blocks, resulting in a model with constant width throughout all layers. The architecture is further simplified by removing the need for special tokens. We evaluate PlainMamba on a variety of visual recognition tasks including image classification, semantic segmentation, object detection, and instance segmentation. Our method achieves performance gains over previous non-hierarchical models and is competitive with hierarchical alternatives. For tasks requiring high-resolution inputs, in particular, PlainMamba requires much less computing while maintaining high performance. Code and models are available at <https://github.com/ChenhongyiYang/PlainMamba>

1 Introduction

Developing high-performing visual encoders has always been one of the most important goals in computer vision [23, 24, 39, 59, 73, 80, 95]. With high-quality visual features, a broad range of downstream tasks, such as semantic segmentation [12, 84, 94, 107], object recognition [39, 60, 80, 95] and detection [38, 53, 67] can be tackled with relative ease.

Early methods for extracting visual representations relied on hand-crafted features such as SIFT [61] and SURF [4]. A big breakthrough then came with the adoption of convolutional neural networks (CNNs) that process images with local contexts and enforce spatial equivariance [39, 47, 73]. Recently, vision

^{*} Equal Contribution

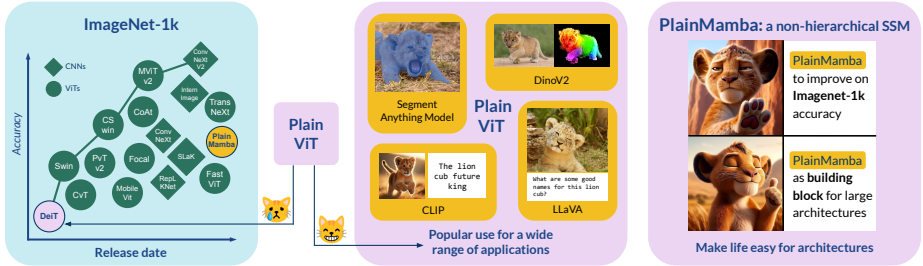


Fig. 1: While hierarchical visual encoders may demonstrate superior accuracy on open-source visual recognition benchmarks, the plain non-hierarchical models have had more widespread use because of their simple structure. In this work, we investigate the potential of the plain Mamba model in visual recognition. *Please note that the presence of lions in this figure is purely due to the first author’s predilection for cats, and is not in any way related to a former name (‘Simba’) of our model.*

transformers (ViTs) [24] obviated the need for such enforced inductive biases in favour of learnable contexts that operate on image patches [59, 80, 82]. However, despite the overwhelming success of transformers and their self-attention mechanism [8, 21, 100], the quadratic cost of attention has proved to be an obstacle to further scaling such models.

This has invigorated interest in state space models (SSMs) [31, 34, 58, 90, 108]. Due to their close ties to linear recurrent networks, SSMs have the benefits of potentially infinite context lengths while maintaining linear complexity in the input sequence length [31], offering substantial speedups compared to attention. However, it took several notable advances to make SSMs effective at learning competitive representations, including enforcing state space variables to be orthogonal basis projections [34]. The recent Mamba [31] architecture further aligned SSM-based models with modern transformers, such as making the state space variables input-dependent — much like queries, keys and values in self-attention. When being used for NLP, those designs led to a state space model that could scale to the sizes and performances of modern transformer-based LLMs [8, 81], while improving long-range context and inference speed.

There is now understandable interest in adapting the Mamba architecture to the visual domain [49, 58, 108]. However, before we start doing that, we need to think about under what guidelines should we design our new model. As we show in Figure 1, by examining the development of recently proposed visual encoders, we find that adding more inductive biases, e.g., hierarchical structure, to the plain model such as DeiT can indeed improve a model’s performance on open-source benchmarks like ImageNet. However, we should not ignore the fact that the plain ViT [24] is widely used by several popular vision foundation models [1, 46, 56, 63, 65], which suggests that simplicity in architecture design is key for multiple reasons. Firstly, maintaining a constant model width (i.e. non-hierarchical) makes it much easier to integrate features from multiple levels, as is common in dense prediction tasks such as semantic segmentation [46]. It also becomes easier to combine features across different modalities such as in

CLIP [65] or LLaVa [56] or as parts of increasingly complex AI-powered systems. Furthermore, simpler components can be more easily optimized for hardware acceleration [17]. In addition, it has also been observed that the over-crafted models may lead to a significant gap between the performance on commonly used benchmarks and downstream tasks [6, 26]. This means benchmark performance may no longer reflect real-world usefulness, as over-engineering tends to increase model complexity and thus make it harder for others to re-use.

Motivated by the above findings, we propose **PlainMamba**: a simple Mamba architecture for visual recognition. This model integrates ideas from CNNs, Transformers and novel SSM-based models with an aim to providing easy-to-use models for the vision modality. Compared to previous visual state space models [58, 108], we simplify the architecture by maintaining constant model width across all layers of the network via stacking identical blocks as well as removing the need for CLS tokens. This allows for easy scaling and model re-use, while achieving competitive performances.

Our contributions are as follows:

- We propose a new visual state space model we call **PlainMamba**. This architecture improves and simplifies previous attempts at extending the Mamba architecture to the visual modality.
- We improve the SSM block by adapting selective scanning to better process 2D spatial inputs, in two ways. (i) Our **continuous 2D scanning** approach ensures that the scanning sequence is spatially continuous to improve semantic continuity. (ii) Our **direction-aware updating**, inspired by positional encoding, allows the model to encode the directionality of each scanning order to further improve spatial context.
- We test our **PlainMamba** architecture using three different sizes (7M, 26M and 50M) and show how they perform competitively on a range of tasks, from ImageNet1K classification to semantic segmentation and object detection. Specifically, we show that PlainMamba outperforms its non-heretical counterparts, including SSMs and Transformers, while performing on par with the hierarchical competitors.

2 Related Work

Visual Feature Extractors How to effectively extract visual features from images has been a long-standing challenge in computer vision. In the early years of deep learning, CNNs [39, 47, 73, 95] dominated the model architecture landscape. Their induced spatial prior, through the use of convolutional filters, exploits the locality of visual features. Furthermore, stacking multiple layers increases their receptive field. Many different CNN backbone architectures have been proposed over the years [13, 44, 47], introducing new ways of exploiting spatial information [73, 95], building deeper models [39, 77], improving efficiency [66, 71, 78], adding multi-scale connections [69], scaling architectures [91], and introducing attention mechanisms [5, 10, 42, 75, 83, 85]. In recent years, ViTs have become a powerful tool for image modeling [24]. Compared to CNNs, they make fewer

assumptions about data (feature locality [98], translation and scale invariance). By replacing the convolutional layers with self-attention modules, transformers can capture global relationships and have achieved state-of-the-art results on many common image benchmarks [20, 54, 107]. To adapt the original transformer architecture [82] for vision tasks, images are split into patches and converted into tokens before being fed into the transformer encoder. Within this framework, numerous works have focused on pushing the performance (e.g. LeViT, [30] combining transformer encoder layers and convolutions), or on reducing the costly quadratic complexity of self-attention [16, 18]. Another popular extension to ViT architectures has been the addition of hierarchical structures [27, 59, 86, 92, 97], similar to the multi-scale feature pyramids used in CNNs. The Swin Transformer [59], for instance, uses shifted windows to share feature information across scales. These multi-scale features are then used for a wide range of downstream tasks. Recent research has explored ways of using these hierarchical features within ViTs themselves [9, 23, 25, 36, 37, 48, 51, 68, 72]. Some works [59] have examined the use of multi-resolution features as attention keys and values to learn multi-scale information. However, these extensions add complexity to the model and make it harder to effectively use its features in later stages, thus hindering widespread adoption. Indeed, recent works [50, 100] return to the original ViT architecture, as its non-hierarchical nature greatly simplifies the use of its features. In particular, the plain ViT provides greater flexibility for pre-training and fine-tuning on different tasks.

State Space Models State Space Models (SSMs) have emerged as efficient alternatives to transformers and CNNs due to their ability to scale linearly with sequence length [33, 76]. SSMs transform the state space to effectively capture dependencies over extended sequences. To alleviate the initial computational cost of such models, S4 [32] enforced low-rank constraints on the state matrix and S5 [74] introduced parallel scanning to further improve efficiency. Furthermore, H3 [29] achieved competitive results on common benchmarks by improving the hardware utilization. Lastly, Mamba [31] parameterized the SSM matrices as functions of the input, thus allowing it to act as a learnable selection mechanism and providing greater flexibility. Follow-up works have extended selective SSMs for images [3, 57, 70, 88, 89] and videos [62] using a hierarchical structure [58] and bidirectional blocks [108], while Mamba-ND [49] introduces an architecture for multi-dimensional data. MambaIR [35] tackles image restoration, and Pan-Mamba [40] works on pan-sharpening. DiS [28] introduces SSMs to diffusion models by replacing the U-Net with an SSM backbone. While drawing inspiration from the above works, PlainMamba improves Mamba’s [31] selective SSM block by adding wider depth-wise convolutions. In contrast to the Cross-Scan Module (CSM) [58] and Mamba-ND [49], PlainMamba respects the spatio-sequential nature of image patches (see Figure 2). As opposed to [108], we do not use the CLS token.

Simplifying Visual Feature Extractors Simplifying and unifying existing methods is equally important as improving performance. Plain non-hierarchical architectures are robust, conceptually simpler, and scale better. In addition, they serve as a basis for future research. ViTs [24] remove the pyramid structure of CNNs by converting images into patched tokens. This way, they easily adapt the transformer architecture for visual tasks. Another trick that stems from sequence modeling is the usage of CLS tokens for prediction, which have proven to be unnecessary for visual tasks [103]. FlexiVit [7] unified into a single architecture images with different input resolutions, and GPViT [100] improved feature resolution with a non-hierarchical transformer. Similarly, ConvNext [60] introduced a simple CNN model that competed with state-of-the-art transformer methods. Other works, like MLP-Mixer [79] and follow-up works [41], have introduced simple architectures using only multi-layer perceptrons. The plain non-hierarchical ViT [24] has served as a simple building block for many diverse tasks. SAM [46] uses a pre-trained ViT as image encoder with minimal changes for image segmentation at large scale. DinoV2 [19, 63] uses a ViT to learn general-purpose visual features by pretraining models on curated datasets with self-supervision. Similarly, the image encoder for the CLIP [65] model consists of a basic ViT with minor modifications, allowing image-text representations to be learned with a contrastive objective. DALLE-2 [1] incorporates a ViT image encoder to extract visual features that are used for text-conditional image generation. LLaVA [55, 56] combines a vision encoder (pretrained ViT from CLIP) and an LLM for vision-language tasks. Inspired by the versatility and flexibility of ViT, this work aims to continue in the direction of simplifying feature extractors while maintaining strong performance by introducing **PlainMamba**: a Simple Mamba architecture.

3 Method

In this section, we introduce PlainMamba in detail. An overview of the proposed model is presented in Figure 2 (a). In Section 3.1, we revisit the background of State Space Modeling and Mamba. Then, we introduce our model architecture and block architecture in Section 3.2 and Section 3.3, respectively. Finally, in Section 3.4, we present different variants of PlainMamba.

3.1 Preliminaries

State Space Models. SSMs are typically used to model a continuous linear time-invariant (LTI) system [90] where an input signal $x(t) \in \mathbb{R}$ is mapped to its output signal $y(t) \in \mathbb{R}$ through a state variable $h(t) \in \mathbb{R}^m$ with the following rules:

$$h'(t) = \mathbf{A}h(t) + \mathbf{B}x(t), \quad y(t) = \mathbf{C}h'(t) + \mathbf{D}x(t) \quad (1)$$

where $\mathbf{A} \in \mathbb{R}^{m \times m}$, $\mathbf{B} \in \mathbb{R}^{m \times 1}$, $\mathbf{C} \in \mathbb{R}^{1 \times m}$ and $\mathbf{D} \in \mathbb{R}^{1 \times 1}$ are parameters.

To make the above system usable for a discrete system, e.g., a sequence-to-sequence task, a timescale parameter Δ is used to transform the parameters \mathbf{A} and \mathbf{B} to their discretized counterparts $\bar{\mathbf{A}}$ and $\bar{\mathbf{B}}$. In Mamba [31] and its following works [58, 108], this is achieved with the following zero-order hold (ZOH) rule:

$$\bar{\mathbf{A}} = \exp(\Delta\mathbf{A}), \quad \bar{\mathbf{B}} = (\Delta\mathbf{A})^{-1}(\exp(\Delta\mathbf{A}) - \mathbf{I}) \cdot \Delta\mathbf{B} \quad (2)$$

Afterwards, an input sequence $\{x_i\}$ (for $i = 1, 2, \dots$) can be mapped to its output sequence $\{y_i\}$ in a similar way:

$$h'_i = \bar{\mathbf{A}}h_{i-1} + \bar{\mathbf{B}}x_i, \quad y_i = \mathbf{C}h'_i + \mathbf{D}x_i \quad (3)$$

Mamba. Since SSMs are often used to model LTI systems, their model parameters are shared by all time steps i . However, as found in Mamba [31], such time-invariant characteristics severely limit the model’s representativity. To alleviate this problem, Mamba lifts the time-invariant constraint and makes the parameters \mathbf{B} , \mathbf{C} and Δ dependent on the input sequence $\{x_i\}$, a process they refer to as the *selective scan*, resulting in the token-dependent $\{\mathbf{B}_i\}$, $\{\mathbf{C}_i\}$ and $\{\Delta_i\}$. Moreover, the SSM is combined with a gated MLP [43] to gain better representation ability. Specifically, the output sequence $\{y_i\}$ is computed from the $\{x_i\}$ as the following⁴:

$$x'_i = \sigma(\text{DWConv}(\text{Linear}(x_i))), \quad z_i = \sigma(\text{Linear}(x_i)) \quad (4)$$

$$\mathbf{B}_i, \mathbf{C}_i, \Delta_i = \text{Linear}(x'_i), \quad \bar{\mathbf{A}}_i, \bar{\mathbf{B}}_i = \text{ZOH}(\mathbf{A}, \mathbf{B}_i, \Delta_i) \quad (5)$$

$$h'_i = \bar{\mathbf{A}}_i h_{i-1} + \bar{\mathbf{B}}_i x'_i, \quad y'_i = \mathbf{C}_i h'_i + \mathbf{D} x'_i, \quad y_i = y'_i \odot z_i \quad (6)$$

where σ denotes the SiLU activation, and \odot denotes element-wise multiply.

3.2 Overall architecture of PlainMamba

In Figure 2, we present the model architecture of PlainMamba. Our model is divided into three main components: (1) a convolutional tokenizer that transforms an input 2D image into a sequence of visual tokens, (2) the main network with a series of L identical PlainMamba blocks to learn high-quality visual representations; and (3) a task-specific head for different types of downstream tasks.

In more detail, the tokenizer will downsample the input image $I \in \mathbb{R}^{H_I \times W_I \times 3}$ into a list of visual tokens $x \in \mathbb{R}^{H \times W \times C}$, where C is the channel number. We set the default down-sampling factor to 16, following ViT [24]. After combining the initial visual tokens with positional embeddings [82] for retaining spatial information, the tokens undergo a series of transformations through the L PlainMamba blocks, which are designed to simplify usage by maintaining the

⁴ For simplicity, here we assume x_i to have a single channel. It is straightforward to modify the formulation for the multi-channel case. The output linear projection that maps the features to their original dimension is also omitted here.

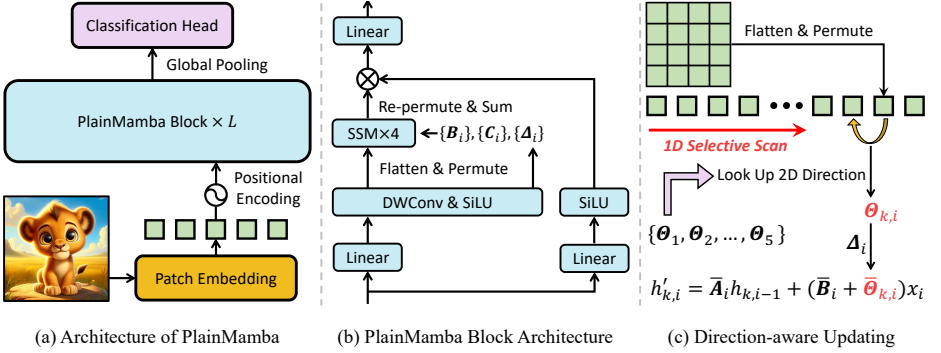


Fig. 2: (a) The overall architecture of the proposed PlainMamba. PlainMamba does not have a hierarchical structure, it instead stacks L identical PlainMamba block to form the main network. For image classification, it uses global average pooling instead of the CLS to gather global information. (b) Architecture of PlainMamba block, which is similar to the Mamba [31] block where the selective scanning is combined with a gated MLP. (c) The proposed *Direction-Aware Updating*, where a series of learnable parameters Θ_k are combined with the data-dependent updating parameters to explicitly inject relative 2D positional information into the selective scanning process.

input-output shape consistency. The final stage of the architecture involves a task-specific head, which is dependent on the particular downstream application. For instance, in image classification tasks, the image tokens are globally pooled into a vector, which is then fed into a linear classification head to produce the final output.

PlainMamba distinguishes itself from existing vision transformers [24, 57] and concurrent vision Mamba [58, 108] architectures in several key aspects. Firstly, it does not use any special tokens, such as the commonly used CLS token. Secondly, in contrast to approaches that adopt a hierarchical structure to manage feature resolution [51, 59, 87], Instead, PlainMamba maintains a constant feature resolution across all blocks. This design choice considers the recent progress made in various visual foundation models [46, 63, 65] where the plain non-hierarchical ViT is used rather than its hierarchical counterparts.

3.3 PlainMamba Block

The overall PlainMamba architecture is comprised of several identical PlainMamba blocks, which form the backbone for learning high-quality visual features. We present the structure of the PlainMamba block in Figure 2. We take inspiration from the original Mamba block where the SSM is combined with a gated MLP in a unified module. However, we make several key adjustments to the selective scanning process to fully exploit the two-dimensional nature of image inputs. This adaptation is crucial for effectively transitioning from the inherently 1D processing paradigm of language models to the 2D domain of images. To this end, we introduce two novel techniques: (1) *Continuous 2D Scanning* and (2) *Direction-Aware Updating*. The first technique ensures that each visual token is

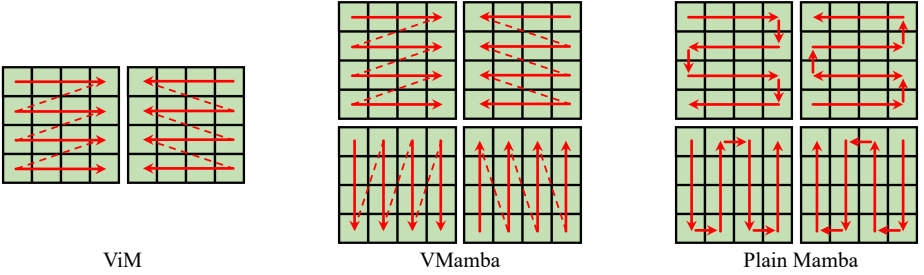


Fig. 3: Comparison between our Continuous 2D Scanning and the selective scan orders in ViM [108] and VMamba [58]. Our method makes sure that every scanned visual token is spatially adjacent to its predecessor, avoiding potential spatial and semantic discontinuity.

always adjacent to the previous scanned token. By doing so, it mitigates positional bias and encourages a more uniform understanding of the image space, enhancing the model’s ability to learn from visual inputs. The second technique explicitly embeds the 2D relative positional information into the selective scanning process, which allows the model to better interpret the positional context of flattened visual tokens.

Continuous 2D Scanning The selective scan mechanism is inherently designed for sequential data, such as text. Adapting this mechanism for 2D image data requires flattening the 2D visual tokens into a 1D sequence to apply the State Space Model (SSM) updating rule. Prior research, e.g., VisionMamba [108] and VMamba [58], has demonstrated the efficacy of using multiple scanning orders to enhance model performance — such as both row-wise and column-wise scans in multiple directions. However, as shown in Figure 3 (a) and (b), in these approaches, each scanning order can only cover one type of 2D direction, e.g., left to right, causing spatial discontinuity when moving to a new row (or column). Moreover, as the parameter \mathbf{A} in Equation 3 serves as a decaying term, such spatial discontinuity can also cause adjacent tokens to be decayed to different degrees, compounding the semantic discontinuity and resulting in potential performance drop.

Our *Continuous 2D Scanning* addresses this challenge by ensuring a scanned visual token is always adjacent (in the 2D space) to the previously scanned token. As shown in Figure 3 (c), in our approach, the visual tokens are also scanned in four distinct orders. When reaching the end of a row (or column), the next scanned token will be its adjacent, *not the opposite*, token in the next column (or row). Then, the scanning continues with a reversed direction until it reaches the final visual token of the image. As a consequence, our method preserves spatial and semantic continuity and avoids potential information loss when scanning non-adjacent tokens. Furthermore, in practice the model usually takes input images of the same size, meaning our method can be easily implemented and efficiently run by pre-computing the permutation indexes.

Table 1: PlainMamba variants. FLOPs are measured using input size 224×224 .

Model	Depth	Channels	Params	FLOPs
PlainMamba-L1	24	192	7.3M	3.0G
PlainMamba-L2	24	384	25.7M	8.1G
PlainMamba-L3	36	448	50.5M	14.4G

Direction-Aware Updating As shown in Equation 3, the contribution of a token x_i to the hidden state h_i in the selective scan is determined by the parameter $\bar{\mathbf{B}}_i$, derived from x_i itself. In language models, the sequential order naturally dictates the positional relationship between tokens, allowing the model to "remember" their relative positions. However, in our Continuous 2D Scanning, the current token can be in one of four possible directions relative to its predecessor. This challenges the model's ability to discern the precise spatial relationship between consecutive tokens based on \mathbf{B}_i alone.

Our *Direction-Aware Updating* is therefore proposed to address this challenge. Drawing inspiration from the relative positional encoding mechanisms in vision transformers [24], we employ a set of learnable parameters $\{\Theta_k \in \mathbb{R}^{m \times 1}\}$ (for $k = 1, 2, \dots, 5$), representing the four cardinal directions plus a special BEGIN direction for the initial token. These parameters are summed with the data-dependent \mathbf{B}_i to enrich the selective scan process with directional information. Specifically, with x_i and z_i following Equation 3, our *Direction-Aware Updating* is formulated as follows:

$$h'_{k,i} = \bar{\mathbf{A}}_i h_{k,i-1} + (\bar{\mathbf{B}}_i + \bar{\Theta}_{k,i}) x_i \quad (7)$$

$$y'_i = \sum_{k=1}^4 (\mathbf{C}_i h'_{k,i} + \mathbf{D} x_i), \quad y_i = y'_i \odot z_i \quad (8)$$

where k spans the four distinct scanning directions introduced by our *Continuous 2D Scanning*. Alternatively, for the initial token of each scan, we instead add the final $\Theta_{k=5}$ vector. The term $\bar{\Theta}_{k,i}$ represents the discretized $\Theta_{k,i}$ using Δ_i .

3.4 Model Variants of PlainMamba

We present three different model variants of PlainMamba. We report their architectural details in Table 1. Specifically, from PlainMamba-L1 to PlainMamba-L2, we scale the model width, i.e., feature channel numbers, and keep the model depth to 24. From PlainMamba-L2 to PlainMamba-L3, we scale both model width and depth. The FLOPs are measured using 224×224 inputs, and we follow the official Mamba codebase to compute the FLOPs of the selective scan process.

4 Experiments

4.1 ImageNet-1K Classification

Setting: We build our codebase following [100]. Specifically, for the ImageNet-1k experiments, we train all PlainMamba models for 300 epochs using AdamW optimizer. Following [59], we set the batch size to 2048, weight decay to 0.05, and the peak learning rate to 0.002. Cosine learning rate scheduling is used. For

data augmentation, we used the commonly used recipe [22, 23, 59, 80], which includes Mixup [104], Cutmix [102], Random erasing [106] and Rand augment [15].

Results: In Table 2, we report the ImageNet-1K experiment results. We compare PlainMamba with three different kinds of visual feature extractors: CNNs, vision transformers, and SSMs. In addition, the comparison includes both hierarchical and non-hierarchical models. Firstly, when comparing with SSMs, our model is doing better than the recently proposed Vision Mamba [108] and Mamba-ND [49]. For example, PlainMamba-L2 achieves a 2.4% higher accuracy than Mamba-ND-T while they share a similar model size. These results validate PlainMamba’s effectiveness as a non-hierarchical SSM. Secondly, when compared with CNNs and transformers, our model achieves better performance than the non-hierarchical counterparts. For example, PlainMamba-L2 achieves 1.7% better accuracy with DeiT-Small. Moreover, PlainMamba also achieves similar performance when compared with hierarchical models. For example, when the model size is around 25M, our model achieves 0.3% better accuracy than Swin-Tiny, validating PlainMamba’s ability as a general feature extractor. On the other hand, the hierarchical VMamba [58], together with other hierarchical transformers, do achieve a better accuracy than ours. As we explained in Section 1, hierarchical models tend to perform better than non-hierarchical ones in visual recognition. As the main motivation of our work is to develop a simple Mamba architecture, a bit inferior ImageNet accuracy is acceptable.

Table 2: Comparison between PlainMamba and other models on ImageNet-1K. (* denotes best epoch result.)

Model	Hierarchical	Params	FLOPs	Top-1
CNN				
ResNeXt101-32×4 [96]	✓	44M	8.0G	78.6
ResNeXt101-32×8 [96]	✓	88M	16.5G	79.3
RegNetY-4G [66]	✓	21M	4.0G	80.0
RegNetY-8G [66]	✓	39M	8.0G	81.7
ConvNeXt-T [60]	✓	29M	4.5G	82.1
ConvNeXt-S [60]	✓	50M	8.7G	83.1
Transformer				
DeiT-Tiny [80]	✗	5M	1.3G	72.2
DeiT-Small [80]	✗	22M	4.6G	79.9
DeiT-Base [80]	✗	86M	16.8G	81.8
Swin-Tiny [59]	✓	29M	4.5G	81.3
Swin-Small [59]	✓	50M	8.7G	83.0
PVT-Tiny [86]	✓	13M	2G	75.1
PVT-Small [86]	✓	25M	3.8G	79.8
PVT-Medium [86]	✓	44M	6.7G	81.2
Focal-Tiny [101]	✓	29M	4.9G	82.2
Focal-Small [101]	✓	51M	9.1G	83.5
State Space Modeling				
ViM-T [108]	✗	7M	-	76.1
ViM-S [108]	✗	26M	-	80.5
LocalViM-T [45]	✗	8M	1.5G	76.2
LocalViM-S [45]	✗	28M	4.8G	81.2
Mamba-ND-T [49]	✗	24M	-	79.2
Mamba-ND-S [49]	✗	63M	-	79.4
S4ND-ViT-B [62]	✗	89M	-	80.4
S4ND-ConvNeXt-T [62]	✓	30M	-	82.2
VMamba-T [58]	✓	22M	5.6G	*82.2
VMamba-S [58]	✓	44M	11.2G	*83.5
PlainMamba-L1	✗	7M	3.0G	77.9
PlainMamba-L2	✗	25M	8.1G	81.6
PlainMamba-L3	✗	50M	14.4G	82.3

4.2 COCO object detection and instance segmentation

Setting: Following [100], we test PlainMamba’s ability on COCO object detection and instance segmentation using both the two-stage Mask R-CNN [38] and the single-stage RetinaNet [53]. For both models, we report the results of both 1× schedule. Following [100], we use ViTAdapter [11] to compute multi-scale features to fit the FPN network structure. We use the commonly used training settings proposed in [59] to keep a fair comparison.

Table 3: Mask R-CNN object detection and instance segmentation on MS COCO *mini-val* using $1\times$ schedule. We use ViTAdapter [11] to compute multi-scale features. FLOPs are computed using input size 1280×800 .

Backbone		Hierarchical Params	FLOPs	AP^{bb}	AP_{50}^{bb}	AP_{75}^{bb}	AP^{mk}	AP_{50}^{mk}	AP_{75}^{mk}
CNN									
ResNeXt101-32x4d [96]	✓	63M	340G	41.9	-	-	37.5	-	-
ResNeXt101-64x4d [96]	✓	102M	493G	42.8	-	-	38.4	-	-
Transformer									
ViT-Adapter-T [11]	✗	29M	349G	41.1	62.5	44.3	37.5	59.7	39.9
ViT-Adapter-S [11]	✗	49M	463G	44.7	65.8	48.3	39.9	62.5	42.8
ViT-Adapter-B [11]	✗	131M	838G	47.0	68.2	51.4	41.8	65.1	44.9
PVT-Small [86]	✓	44M	-	40.4	62.9	43.8	37.8	60.1	40.3
PVT-Medium [86]	✓	64M	-	42.0	64.4	45.6	39.0	61.6	42.1
PVT-Large [86]	✓	81M	-	42.9	65.0	46.6	39.5	61.9	42.5
Swin-Tiny [59]	✓	48M	264G	42.2	-	-	39.1	-	-
Swin-Small [59]	✓	69M	354G	44.8	-	-	40.9	-	-
ViL-Tiny [105]	✓	26M	145G	41.4	63.5	45.0	38.1	60.3	40.8
ViL-Small [105]	✓	45M	218G	44.9	67.1	49.3	41.0	64.2	44.1
ViL-Medium [105]	✓	60M	293G	47.6	69.8	52.1	43.0	66.9	46.6
State Space Modeling									
EfficientVMamba-T [64]	✓	11M	60G	35.6	57.7	38.0	33.2	54.4	35.1
EfficientVMamba-S [64]	✓	31M	197G	39.3	61.8	42.6	36.7	58.9	39.2
EfficientVMamba-B [64]	✓	53M	252G	43.7	66.2	47.9	40.2	63.3	42.9
VMamba-T [58]	✓	42M	262G	46.5	68.5	50.7	42.1	65.5	45.3
VMamba-S [58]	✓	64M	357G	48.2	69.7	52.5	43.0	66.6	46.4
PlainMamba-Adapter-L1	✗	31M	388G	44.1	64.8	47.9	39.1	61.6	41.9
PlainMamba-Adapter-L2	✗	53M	542G	46.0	66.9	50.1	40.6	63.8	43.6
PlainMamba-Adapter-L3	✗	79M	696G	46.8	68.0	51.1	41.2	64.7	43.9

Results: We report the results of Mask R-CNN object detection and instance segmentation in Table 3 and RetinaNet object detection in Table 4. For Mask R-CNN, PlainMamba is on par with the state-of-the-art architectures. For example, with similar FLOPs and many fewer parameters, PlainMamba-L1 achieves 44.1 AP^{bb} and 39.1 AP^{mk} when using $1\times$ training schedule, while Swin-Small achieves 44.8 AP^{bb} and 40.9 AP^{mk} . We also observe that hierarchical models tend to work better than non-hierarchical models. Although our model achieves lower performance than some hierarchical models, e.g., the concurrent VMamba [58], PlainMamba achieves the best performance among its non-hierarchical counterparts. For instance, when using $1\times$ training schedule, PlainMamba achieves 3.1 higher AP^{bb} and 1.6 higher AP^{mk} than DeiT-T when they are both equipped with the ViTAdapter [11]. These results demonstrate that PlainMamba is able to extract good local features, which is important to the object-level tasks like instance segmentation. Similarly, PlainMamba also

Table 4: RetinaNet object detection on MS COCO *mini-val* with $1\times$ schedule. FLOPs are computed using input size 1280×800 .

Backbone		Hierarchical Params	FLOPs	AP^{bb}	AP_{50}^{bb}	AP_{75}^{bb}
CNN						
ResNeXt101-32x4d [96]	✓	56M	319G	39.9	-	-
ResNeXt101-64x4d [96]	✓	95M	413G	41.0	-	-
Transformer						
Swin-Tiny [59]	✓	38M	245G	41.5	-	-
Swin-Small [59]	✓	60M	335G	44.5	-	-
Focal-Tiny [101]	✓	39M	265G	43.7	-	-
Focal-Small [101]	✓	62M	367G	45.6	-	-
PVT-Small [86]	✓	34M	-	40.4	61.3	43.0
PVT-Medium [86]	✓	54M	-	41.9	63.1	44.3
PVT-Large [86]	✓	71M	-	42.6	63.7	45.4
State Space Modeling						
EfficientVMamba-T [64]	✓	13M	-	37.5	57.8	39.6
EfficientVMamba-S [64]	✓	19M	-	39.1	60.3	41.2
EfficientVMamba-B [64]	✓	44M	-	42.8	63.9	45.8
PlainMamba-Adapter-L1	✗	19M	250G	41.7	62.1	44.4
PlainMamba-Adapter-L2	✗	40M	392G	43.9	64.9	47.0
PlainMamba-Adapter-L3	✗	67M	478G	44.8	66.0	47.9

Table 5: ADE20K semantic segmentation using UperNet. The FLOPs are computed using input size 512×2048 . PlainMamba has much smaller FLOPs here because we used feature maps in a constant resolution of 16.

Backbone	Hierarchical	Params	FLOPs	mIoU
CNN				
ResNet-50 [39]	✓	67M	953G	42.1
ResNet-101 [39]	✓	85M	1030G	44.0
ConvNeXt-T [60]	✓	60M	939G	46.7
Transformer				
DeiT-S+MLN [80]	✗	58M	1217G	43.8
DeiT-B+MLN [80]	✗	144M	2007G	45.5
XCiT-T12/8 [2]	✗	34M	-	43.5
XCiT-S12/8 [2]	✗	52M	1237G	46.6
XCiT-S24/8 [2]	✗	74M	1587G	48.1
Swin-Tiny [59]	✓	60M	945G	44.5
Swin-Small [59]	✓	81M	1038G	47.6
Focal-Tiny [101]	✓	62M	998G	45.8
Focal-Small [101]	✓	85M	1130G	48.0
Twins-SVT-Small [14]	✓	54M	912G	46.2
Twins-SVT-Small [14]	✓	88M	1044G	47.7
State Space Modeling				
ViM-T [108]	✗	13M	-	41.0
ViM-S [108]	✗	46M	-	44.9
LocalViM-T [45]	✗	36M	181G	43.4
LocalViM-S [45]	✗	58M	297G	46.4
VMamba-T [58]	✓	55M	964G	47.3
VMamba-S [58]	✓	76M	1081G	49.5
PlainMamba-L1	✗	35M	174G	44.1
PlainMamba-L2	✗	55M	285G	46.8
PlainMamba-L3	✗	81M	419G	49.1

performs well with the single-stage RetinaNet object detector. For example, with only half the model size and similar FLOPs, PlainMamba-L1 achieves 0.2 higher AP than Swin-Tiny. On the other hand, we also admit that PlainMamba is performing worse than the hierarchical VMamba [58]. We attribute such inferiority to the multi-resolution architecture of FPN-based [52] Mask R-CNN, which is more naturally suitable to the hierarchical designs.

4.3 ADE20K Semantic Segmentation

Setting: We follow common practice [23, 59, 100] and benchmark PlainMamba’s ability on semantic segmentation with UperNet [94] as the segmentation network. Unlike XCiT [2], we do not explicitly resize the constant resolution feature maps into multi-scale. Following [59], we train all models for 160 iterations with batch size 16 and set the default training image size to 512×512 .

Results: We report our model’s ADE20K semantic segmentation performance in Table 5. Similar to the ImageNet-1k and COCO experiments, here the competing models include both hierarchical and non-hierarchical backbones in three types of visual feature extractors. The results again suggest that PlainMamba achieves the best performance among the non-hierarchical models. For example, with similar parameter amounts, PlainMamba-L2 outperforms the high-resolution (patch size

of 8) XCiT-S12/8 model [2] with a much lower computation cost. Moreover, PlainMamba-L2 also outperforms the hierarchical Swin-Transformer-Tiny [59], achieving better mIoU while having a lower model size and FLOPs. At the same time, PlainMamba is also doing better than the concurrent Vision Mamba [108]. For instance, PlainMamba-L2 achieves a 1.9 higher mIoU than ViM-S. This result verifies our model’s effectiveness in extracting fine-grained visual features, which is essential for the pixel-wise semantic segmentation task.

4.4 Ablation Studies and Discussions

Setting: Here, we conduct ablation studies to test our model designs and to gain a deeper understanding of the proposed method. We use our L1 model, with less than 10M parameters, for most experiments. The models are all pre-trained on ImageNet-1K following the same training settings described in Section 4.1.

Table 6: Ablation study of model depth v.s. width on ImageNet-1K.

Depth	Width	Params	FLOPs	Top-1
6	376	7.3 M	2.5 G	74.6
12	272	7.5 M	2.7 G	76.8
24	192	7.3 M	3.0 G	77.9
36	156	7.2 M	3.3 G	77.9

Depth v.s. Width When designing neural architectures for a given parameter count, it’s usually important to find a good balance between the network’s depth, i.e., the number of layers, and its width, i.e., the feature dimensions. While this problem was studied for existing architectures [93, 99], it is still unclear whether the previous conclusions are applicable to vision SSMs. In Table 6, we study the depth and width trade-off of the proposed PlainMamba. Firstly, the results show that deeper models tend to perform better than shallow ones. For example, when the parameter count is around 7.4M, the 12-layer model achieves 2.2% higher ImageNet top-1 accuracy than the 6-layer counterparts, and the 24-layer model is further 1.1% higher than the 12-layer one. However, when we further increase the depth to 36 while reducing the width accordingly, the top-1 accuracy remains similar. On the other hand, we also notice that deeper models are less efficient than shallower but wider models. For instance, the 24-layer model is 0.3G FLOPs higher than the 12-layer model. These results suggest the necessity of a good balance between network depth and width.

PlainMamba Block Design. Here, we test different designs of the PlainMamba block by comparing it with the block designs in Vision Mamba [108] and VMamba [58]. For a fair comparison, we use the same model depth and

Table 7: Ablation study of model depth v.s. width on ImageNet-1K.

Method	Params	FLOPs	Top-1
VisionMamba [108]	7.8M	1.3G	74.4
VMamba [58]	7.3M	3.0G	77.1
Ours	7.3M	3.0G	77.9

width settings for all designs and train all models with the same training recipe. We also remove the CLS tokens from the Vision Mamba [108] block and use the global averaging pooling as an alternative. We report the results in Table 7. We can see that our design achieves the best results. Specifically, Vision Mamba only achieves a 74.4% ImageNet accuracy, which is 3.5% lower than ours. We also

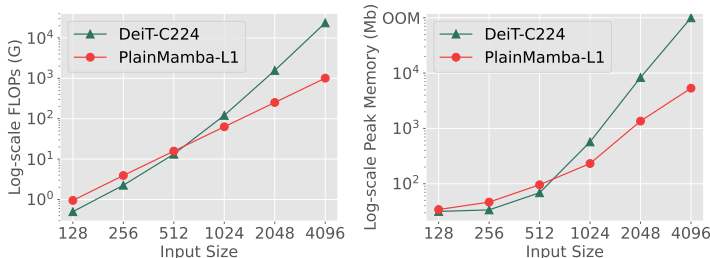


Fig. 4: Efficiency comparison between PlainMamba and DeiT. We modify the DeiT-Tiny model by changing its channel number to 224, resulting in a similar-size model (7.4M) to PlainMamba-L1. The peak memory is measured using a batch size of 1.

notice that the model with a Vision Mamba block is inferior to the original Vision Mamba model, which is caused by the removal of the CLS token. These results suggest that our model still retains its ability when the CLS token is absent. Also, our design performs better than the VMamba block [58] with a 0.8% accuracy advantage, indicating that the improvements come from our proposed Continuous 2D Scanning and Direction-aware Updating, which validate the effectiveness of our proposed techniques in adapting SSM for 2D images.

Efficiency Comparison with ViT

One particular advantage of SSMs, e.g., Mamba, is their ability to capture global information while maintaining efficiency. In Figure 4, we compare the PlainMamba’s efficiency with the vision transformer. Specifically, to ensure a fair comparison, we create a

DeiT model with channel numbers of 224, resulting in a model with 7.4M parameters, which is used to compare with PlainMamba-L1. Specifically, we compare the model FLOPs and the peak inference memory using inputs of different sizes. The results show that our model is able to keep the computation cost low when the input size is scaled up to high resolutions, e.g., 4096×4096 . However, DeiT’s FLOPs and memory consumption increase rapidly when using such high-resolution inputs. On the other hand, we also notice that our model’s efficiency is inferior to the similar-sized DeiT when using low-resolution images, e.g., 128×128 . To further investigate such a difference in their efficiency, we decompose their FLOPs into three parts [79]: 1) *token mixing*, 2) *channel mixing*, and 3) *others*. Specifically, token mixing refers to the multi-head attention part in DeiT and the selective scanning part in PlainMamba, and channel mixing refers to the feed-forward network in DeiT and the input & output projection in PlainMamba. We report the results in Table 8. These suggest that PlainMamba’s FLOPs are evenly distributed across the three parts in low and high resolutions. On the contrary, when using 128×128 inputs, DeiT’s FLOPs are dominated by channel-mixing and the

Table 8: Comparison of decomposed FLOPs between DeiT and PlainMamba.

Resolution	Part	DeiT-C224	PlainMamba-L1
128×128	Token Mixing	0.18G	0.34G
	Channel Mixing	0.31G	0.33G
	Others	0.01G	0.30G
4096×4096	Token Mixing	23244G	350G
	Channel Mixing	315G	348G
	Others	12G	311G

other two parts are negligible. However, because of the quadratic complexity of self-attention operation, DeiT’s FLOPs in token mixing grow to $23T$ when using 4096×4096 inputs, 23 times more expensive than PlainMamba. These results verify PlainMamba’s high efficiency when using high-resolution inputs.

5 Conclusion

In this paper, we present PlainMamba, a plain SSM-based model for visual recognition. Our model is conceptually simple because it does not use any special tokens and does not have a hierarchical structure, making it a perfect counterpart to the widely used plain vision transformer. To better adapt SSM to model 2D visual features, we propose two techniques, namely (i) Continuous 2D Scanning and (ii) Direction-aware updating. We benchmark PlainMamba on a wide range of visual recognition tasks, including image classification, object detection, instance segmentation, and semantic segmentation. The results show that PlainMamba achieves superior performance to previous non-hierarchical models, including the concurrent SSM-based models, and can perform on par with the high-performing hierarchical models. Moreover, when being used for high-resolution inputs, PlainMamba requires significantly less computing compared to the vision transformer. We hope our model can serve as a baseline method for future research in this area.

Acknowledgements

Funding for this research is provided in part by a studentship from the School of Engineering at the University of Edinburgh, the SENSE - Centre for Satellite Data in Environmental Science CDT, and an EPSRC New Investigator Award (EP/X020703/1).

References

1. et al, A.R.: Hierarchical text-conditional image generation with clip latents (2022) [2](#), [5](#)
2. Ali, A., Touvron, H., Caron, M., Bojanowski, P., Douze, M., Joulin, A., Laptev, I., Neverova, N., Synnaeve, G., Verbeek, J., et al.: Xcit: Cross-covariance image transformers. *Advances in neural information processing systems* **34**, 20014–20027 (2021) [12](#), [13](#)
3. Baron, E., Zimerman, I., Wolf, L.: 2-D SSM: A General Spatial Layer for Visual Transformers (2023) [4](#)
4. Bay, H., Tuytelaars, T., Van Gool, L.: SURF: Speeded Up Robust Features (2006) [1](#)
5. Bello, I.: Lambdanetworks: Modeling long-range interactions without attention. In: *International Conference on Learning Representations* (2021), <https://openreview.net/forum?id=xTJEN-gg11b> [3](#)
6. Beyer, L., Hénaff, O.J., Kolesnikov, A., Zhai, X., Oord, A.v.d.: Are we done with imagenet? (2020) [3](#)
7. Beyer, L., Izmailov, P., Kolesnikov, A., Caron, M., Kornblith, S., Zhai, X., Minderer, M., Tschannen, M., Alabdulmohsin, I., Pavetic, F.: FlexiViT: One Model for All Patch Sizes. In: *CVPR* (2023) [5](#)
8. Brown, T., Mann, B., Ryder, N., Subbiah, M., Kaplan, J.D., Dhariwal, P., Nee-lakantan, A., Shyam, P., Sastry, G., Askell, A., Agarwal, S., Herbert-Voss, A., Krueger, G., Henighan, T., Child, R., Ramesh, A., Ziegler, D., Wu, J., Winter, C., Hesse, C., Chen, M., Sigler, E., Litwin, M., Gray, S., Chess, B., Clark, J., Berner, C., McCandlish, S., Radford, A., Sutskever, I., Amodei, D.: Language models are few-shot learners. In: Larochelle, H., Ranzato, M., Hadsell, R., Balcan, M., Lin, H. (eds.) *NeurIPS* (2020) [2](#)
9. Chen, C.F., Panda, R., Fan, Q.: Regionvit: Regional-to-local attention for vision transformers. In: *International Conference on Learning Representations* (2022) [4](#)
10. Chen, Y., Fan, H., Xu, B., Yan, Z., Kalantidis, Y., Rohrbach, M., Yan, S., Feng, J.: Drop an octave: Reducing spatial redundancy in convolutional neural networks with octave convolution. In: *Proceedings of the IEEE/CVF International Conference on Computer Vision*. pp. 3435–3444 (2019) [3](#)
11. Chen, Z., Duan, Y., Wang, W., He, J., Lu, T., Dai, J., Qiao, Y.: Vision transformer adapter for dense predictions. *arXiv preprint arXiv:2205.08534* (2022) [10](#), [11](#)
12. Cheng, B., Misra, I., Schwing, A.G., Kirillov, A., Girdhar, R.: Masked-attention mask transformer for universal image segmentation. In: *Proceedings of the IEEE/CVF Conference on Computer Vision and Pattern Recognition* (June 2022) [1](#)
13. Chollet, F.: Xception: Deep Learning with Depthwise Separable Convolutions. In: *CVPR* (2016) [3](#)
14. Chu, X., Tian, Z., Wang, Y., Zhang, B., Ren, H., Wei, X., Xia, H., Shen, C.: Twins: Revisiting Spatial Attention Design in Vision Transformers. *arXiv.org* (Apr 2021) [12](#)
15. Cubuk, E.D., Zoph, B., Shlens, J., Le, Q.V.: Randaugment: Practical automated data augmentation with a reduced search space. In: *Proceedings of the IEEE/CVF conference on computer vision and pattern recognition workshops*. pp. 702–703 (2020) [10](#)
16. Dao, T.: FlashAttention-2: Faster attention with better parallelism and work partitioning (2024) [4](#)

17. Dao, T., Fu, D., Ermon, S., Rudra, A., Ré, C.: Flashattention: Fast and memory-efficient exact attention with io-awareness. *Advances in Neural Information Processing Systems* **35**, 16344–16359 (2022) [3](#)
18. Dao, T., Fu, D.Y., Ermon, S., Rudra, A., Ré, C.: FlashAttention: Fast and memory-efficient exact attention with IO-awareness. In: *NeurIPS* (2022) [4](#)
19. Darcet, T., Oquab, M., Mairal, J., Bojanowski, P.: Vision transformers need registers (2023) [5](#)
20. Deng, J., Dong, W., Socher, R., Li, L.J., Li, K., Fei-Fei, L.: Imagenet: A large-scale hierarchical image database. In: 2009 IEEE conference on computer vision and pattern recognition. pp. 248–255. Ieee (2009) [4](#)
21. Devlin, J., Chang, M.W., Lee, K., Toutanova, K.: BERT: Pre-training of deep bidirectional transformers for language understanding. In: *Proceedings of the 2019 Conference of the North American Chapter of the Association for Computational Linguistics: Human Language Technologies, Volume 1 (Long and Short Papers)*. pp. 4171–4186. Association for Computational Linguistics, Minneapolis, Minnesota (Jun 2019). <https://doi.org/10.18653/v1/N19-1423>, <https://www.aclweb.org/anthology/N19-1423> [2](#)
22. Ding, M., Xiao, B., Codella, N., Luo, P., Wang, J., Yuan, L.: Davit: Dual attention vision transformers. In: *Proceedings of the European conference on computer vision* (2022) [10](#)
23. Dong, X., Bao, J., Chen, D., Zhang, W., Yu, N., Yuan, L., Chen, D., Guo, B.: Cswin transformer: A general vision transformer backbone with cross-shaped windows. In: *Proceedings of the IEEE/CVF Conference on Computer Vision and Pattern Recognition*. pp. 12124–12134 (June 2022) [1](#), [4](#), [10](#), [12](#)
24. Dosovitskiy, A., Beyer, L., Kolesnikov, A., Weissenborn, D., Zhai, X., Unterthiner, T., Dehghani, M., Minderer, M., Heigold, G., Gelly, S., Uszkoreit, J., Houlsby, N.: An image is worth 16x16 words: Transformers for image recognition at scale. In: *International Conference on Learning Representations* (2021), <https://openreview.net/forum?id=YicbFdNTTy> [1](#), [2](#), [3](#), [5](#), [6](#), [7](#), [9](#)
25. d’Ascoli, S., Touvron, H., Leavitt, M.L., Morcos, A.S., Biroli, G., Sagun, L.: Convit: Improving vision transformers with soft convolutional inductive biases. In: *International Conference on Machine Learning*. PMLR (2021) [4](#)
26. Ericsson, L., Gouk, H., Hospedales, T.M.: How well do self-supervised models transfer? In: *CVPR* (2021) [3](#)
27. Fan, H., Xiong, B., Mangalam, K., Li, Y., Yan, Z., Malik, J., Feichtenhofer, C.: Multiscale vision transformers. In: *Proceedings of the IEEE/CVF International Conference on Computer Vision*. pp. 6824–6835 (2021) [4](#)
28. Fei, Z., Fan, M., Yu, C., Huang, J.: Scalable Diffusion Models with State Space Backbone (2024) [4](#)
29. Fu, D.Y., Dao, T., Saab, K.K., Thomas, A.W., Rudra, A., Ré, C.: Hungry Hungry Hippos: Towards Language Modeling with State Space Models. In: *ICLR* (2023) [4](#)
30. Graham, B., El-Nouby, A., Touvron, H., Stock, P., Joulin, A., Jégou, H., Douze, M.: Levit: A vision transformer in convnet’s clothing for faster inference. In: *Proceedings of the IEEE/CVF International Conference on Computer Vision* (2021) [4](#)
31. Gu, A., Dao, T.: Mamba: Linear-time sequence modeling with selective state spaces. *arXiv preprint arXiv:2312.00752* (2023) [2](#), [4](#), [6](#), [7](#)
32. Gu, A., Goel, K., Ré, C.: Efficiently Modeling Long Sequences with Structured State Spaces. In: *ICLR* [4](#)

33. Gu, A., Johnson, I., Goel, K., Saab, K.K., Dao, T., Rudra, A., Re, C.: Combining Recurrent, Convolutional, and Continuous-time Models with Linear State Space Layers. In: NeurIPS (2021) [4](#)
34. Gu, A., Johnson, I., Timalisina, A., Rudra, A., Ré, C.: How to train your hippo: State space models with generalized orthogonal basis projections. In: ICLR (2023) [2](#)
35. Guo, H., Li, J., Dai, T., Ouyang, Z., Ren, X., Xia, S.T.: MambaIR: A Simple Baseline for Image Restoration with State-Space Model (2024) [4](#)
36. Guo, J., Han, K., Wu, H., Tang, Y., Chen, X., Wang, Y., Xu, C.: Cmt: Convolutional neural networks meet vision transformers. In: Proceedings of the IEEE/CVF Conference on Computer Vision and Pattern Recognition. pp. 12175–12185 (June 2022) [4](#)
37. Hatamizadeh, A., Yin, H., Kautz, J., Molchanov, P.: Global context vision transformers. arXiv preprint arXiv:2206.09959 (2022) [4](#)
38. He, K., Gkioxari, G., Dollar, P., Girshick, R.: Mask r-cnn. In: Proceedings of the IEEE International Conference on Computer Vision (Oct 2017) [1](#), [10](#)
39. He, K., Zhang, X., Ren, S., Sun, J.: Deep Residual Learning for Image Recognition. In: The IEEE Conference on Computer Vision and Pattern Recognition (Jun 2016) [1](#), [3](#), [12](#)
40. He, X., Cao, K., Yan, K., Li, R., Xie, C., Zhang, J., Zhou, M.: Pan-Mamba: Effective pan-sharpening with State Space Model (Feb 2024). <https://doi.org/10.48550/arXiv.2402.12192> [4](#)
41. Hou, Q., Jiang, Z., Yuan, L., Cheng, M.M., Yan, S., Feng, J.: Vision Permutator: A Permutable MLP-Like Architecture for Visual Recognition (2022) [5](#)
42. Hu, J., Shen, L., Sun, G.: Squeeze-and-excitation networks. In: 2018 IEEE/CVF Conference on Computer Vision and Pattern Recognition. pp. 7132–7141 (2018). <https://doi.org/10.1109/CVPR.2018.00745> [3](#)
43. Hua, W., Dai, Z., Liu, H., Le, Q.V.: Transformer Quality in Linear Time (2022) [6](#)
44. Huang, G., Liu, Z., van der Maaten, L., Weinberger, K.Q.: Densely connected convolutional networks. In: CVPR (2017) [3](#)
45. Huang, T., Pei, X., You, S., Wang, F., Qian, C., Xu, C.: Localmamba: Visual state space model with windowed selective scan. arXiv preprint arXiv:2403.09338 (2024) [10](#), [12](#)
46. Kirillov, A., Mintun, E., Ravi, N., Mao, H., Rolland, C., Gustafson, L., Xiao, T., Whitehead, S., Berg, A.C., Lo, W.Y., Dollár, P., Girshick, R.: Segment anything. arXiv:2304.02643 (2023) [2](#), [5](#), [7](#)
47. Krizhevsky, A., Sutskever, I., Hinton, G.E.: Imagenet classification with deep convolutional neural networks. In: NeurIPS (2012) [1](#), [3](#)
48. Lee, Y., Kim, J., Willette, J., Hwang, S.J.: Mpvit: Multi-path vision transformer for dense prediction. In: Proceedings of the IEEE/CVF Conference on Computer Vision and Pattern Recognition. pp. 7287–7296 (June 2022) [4](#)
49. Li, S., Singh, H., Grover, A.: Mamba-nd: Selective state space modeling for multi-dimensional data. arXiv preprint arXiv:2402.05892 (2024) [2](#), [4](#), [10](#)
50. Li, Y., Mao, H., Girshick, R., He, K.: Exploring plain vision transformer backbones for object detection. In: Proceedings of the IEEE conference on computer vision and pattern recognition (2022) [4](#)
51. Li, Y., Wu, C.Y., Fan, H., Mangalam, K., Xiong, B., Malik, J., Feichtenhofer, C.: Mvitv2: Improved multiscale vision transformers for classification and detection. In: Proceedings of the IEEE/CVF Conference on Computer Vision and Pattern Recognition. pp. 4804–4814 (June 2022) [4](#), [7](#)

52. Lin, T.Y., Dollár, P., Girshick, R., He, K., Hariharan, B., Belongie, S.: Feature pyramid networks for object detection. In: Proceedings of the IEEE conference on computer vision and pattern recognition. pp. 2117–2125 (2017) [12](#)
53. Lin, T.Y., Goyal, P., Girshick, R., He, K., Dollar, P.: Focal loss for dense object detection. In: Proceedings of the IEEE International Conference on Computer Vision (Oct 2017) [1](#), [10](#)
54. Lin, T.Y., Maire, M., Belongie, S., Hays, J., Perona, P., Ramanan, D., Dollár, P., Zitnick, C.L.: Microsoft COCO: Common Objects in Context. In: Fleet, D., Pajdla, T., Schiele, B., Tuytelaars, T. (eds.) Proceedings of the European conference on computer vision, pp. 740–755 (2014) [4](#)
55. Liu, H., Li, C., Li, Y., Lee, Y.J.: Improved baselines with visual instruction tuning (2023) [5](#)
56. Liu, H., Li, C., Wu, Q., Lee, Y.J.: Visual instruction tuning. In: NeurIPS (2023) [2](#), [3](#), [5](#)
57. Liu, J., Yang, H., Zhou, H.Y., Xi, Y., Yu, L., Yu, Y., Liang, Y., Shi, G., Zhang, S., Zheng, H., Wang, S.: Swin-UMamba: Mamba-based UNet with ImageNet-based pretraining (2024) [4](#), [7](#)
58. Liu, Y., Tian, Y., Zhao, Y., Yu, H., Xie, L., Wang, Y., Ye, Q., Liu, Y.: Vmamba: Visual state space model. arXiv preprint arXiv:2401.10166 (2024) [2](#), [3](#), [4](#), [6](#), [7](#), [8](#), [10](#), [11](#), [12](#), [13](#), [14](#)
59. Liu, Z., Lin, Y., Cao, Y., Hu, H., Wei, Y., Zhang, Z., Lin, S., Guo, B.: Swin Transformer: Hierarchical Vision Transformer using Shifted Windows. In: Proceedings of the IEEE/CVF International Conference on Computer Vision (2021) [1](#), [2](#), [4](#), [7](#), [9](#), [10](#), [11](#), [12](#), [13](#)
60. Liu, Z., Mao, H., Wu, C.Y., Feichtenhofer, C., Darrell, T., Xie, S.: A ConvNet for the 2020s. In: CVPR (2022) [1](#), [5](#), [10](#), [12](#)
61. Lowe, D.G.: Distinctive image features from scale-invariant keypoints (2004) [1](#)
62. Nguyen, E., Goel, K., Gu, A., Downs, G., Shah, P., Dao, T., Baccus, S., Ré, C.: S4nd: Modeling images and videos as multidimensional signals with state spaces. NeurIPS (2022) [4](#), [10](#)
63. Oquab, M., Darcet, T., Moutakanni, T., Vo, H.V., Szafraniec, M., Khalidov, V., Fernandez, P., Haziza, D., Massa, F., El-Nouby, A., Howes, R., Huang, P.Y., Xu, H., Sharma, V., Li, S.W., Galuba, W., Rabbat, M., Assran, M., Ballas, N., Synnaeve, G., Misra, I., Jegou, H., Mairal, J., Labatut, P., Joulin, A., Bojanowski, P.: Dinov2: Learning robust visual features without supervision (2023) [2](#), [5](#), [7](#)
64. Pei, X., Huang, T., Xu, C.: Efficientvmamba: Atrous selective scan for light weight visual mamba. arXiv preprint arXiv:2403.09977 (2024) [11](#)
65. Radford, A., Kim, J.W., Hallacy, C., Ramesh, A., Goh, G., Agarwal, S., Sastry, G., Askell, A., Mishkin, P., Clark, J., et al.: Learning transferable visual models from natural language supervision. In: ICML (2021) [2](#), [3](#), [5](#), [7](#)
66. Radosavovic, I., Kosaraju, R.P., Girshick, R., He, K., Dollár, P.: Designing network design spaces. In: CVPR (2020) [3](#), [10](#)
67. Ren, S., He, K., Girshick, R., Sun, J.: Faster r-cnn: Towards real-time object detection with region proposal networks. In: NeurIPS (2015) [1](#)
68. Ren, S., Zhou, D., He, S., Feng, J., Wang, X.: Shunted self-attention via multi-scale token aggregation. In: Proceedings of the IEEE/CVF Conference on Computer Vision and Pattern Recognition. pp. 10853–10862 (June 2022) [4](#)
69. Ronneberger, O., Fischer, P., Brox, T.: U-Net: Convolutional Networks for Biomedical Image Segmentation. In: MICCAI (2015) [3](#)
70. Ruan, J., Xiang, S.: VM-UNet: Vision Mamba UNet for Medical Image Segmentation (2024) [4](#)

71. Sandler, M., Howard, A., Zhu, M., Zhmoginov, A., Chen, L.C.: MobileNetV2: Inverted Residuals and Linear Bottlenecks. In: CVPR (2018) [3](#)
72. Shi, D.: TransNeXt: Robust Foveal Visual Perception for Vision Transformers. In: CVPR (2024) [4](#)
73. Simonyan, K., Zisserman, A.: Very deep convolutional networks for large-scale image recognition. In: ICLR (2015) [1](#), [3](#)
74. Smith, J.T.H., Warrington, A., Linderman, S.W.: Simplified State Space Layers for Sequence Modeling. In: ICLR (2023) [4](#)
75. Srinivas, A., Lin, T.Y., Parmar, N., Shlens, J., Abbeel, P., Vaswani, A.: Bottleneck transformers for visual recognition. arXiv preprint arXiv:2101.11605 (2021) [3](#)
76. Sun, Y., Dong, L., Huang, S., Ma, S., Xia, Y., Xue, J., Wang, J., Wei, F.: Retentive Network: A Successor to Transformer for Large Language Models (2023) [4](#)
77. Szegedy, C., Liu, W., Jia, Y., Sermanet, P., Reed, S., Anguelov, D., Erhan, D., Vanhoucke, V., Rabinovich, A.: Going deeper with convolutions. In: CVPR (2015) [3](#)
78. Tan, M., Le, Q.: EfficientNet: Rethinking Model Scaling for Convolutional Neural Networks. In: Chaudhuri, K., Salakhutdinov, R. (eds.) Proceedings of the 36th International Conference on Machine Learning. pp. 6105–6114. PMLR, Long Beach, California, USA (Jun 2019) [3](#)
79. Tolstikhin, I.O., Housley, N., Kolesnikov, A., Beyer, L., Zhai, X., Unterthiner, T., Yung, J., Steiner, A., Keysers, D., Uszkoreit, J., et al.: Mlp-mixer: An all-mlp architecture for vision. Advances in Neural Information Processing Systems **34**, 24261–24272 (2021) [5](#), [14](#)
80. Touvron, H., Cord, M., Douze, M., Massa, F., Sablayrolles, A., Jégou, H.: Training data-efficient image transformers & distillation through attention. In: Proceedings of the 38th International Conference on Machine Learning (2021) [1](#), [2](#), [10](#), [12](#)
81. Touvron, H., Lavril, T., Izacard, G., Martinet, X., Lachaux, M.A., Lacroix, T., Rozière, B., Goyal, N., Hambro, E., Azhar, F., et al.: Llama: Open and efficient foundation language models. arXiv preprint arXiv:2302.13971 (2023) [2](#)
82. Vaswani, A., Shazeer, N., Parmar, N., Uszkoreit, J., Jones, L., Gomez, A.N., Kaiser, u., Polosukhin, I.: Attention is All you Need. In: Guyon, I., Luxburg, U.V., Bengio, S., Wallach, H., Fergus, R., Vishwanathan, S., Garnett, R. (eds.) Advances in Neural Information Processing Systems. Curran Associates, Inc. (2017) [2](#), [4](#), [6](#)
83. Wang, F., Jiang, M., Qian, C., Yang, S., Li, C., Zhang, H., Wang, X., Tang, X.: Residual Attention Network for Image Classification. In: CVPR (2017) [3](#)
84. Wang, K., Kim, D., Feris, R., Betke, M.: Cdac: Cross-domain attention consistency in transformer for domain adaptive semantic segmentation. In: Proceedings of the IEEE/CVF International Conference on Computer Vision. pp. 11519–11529 (2023) [1](#)
85. Wang, Q., Wu, B., Zhu, P., Li, P., Zuo, W., Hu, Q.: Eca-net: Efficient channel attention for deep convolutional neural networks. In: The IEEE Conference on Computer Vision and Pattern Recognition (2020) [3](#)
86. Wang, W., Xie, E., Li, X., Fan, D.P., Song, K., Liang, D., Lu, T., Luo, P., Shao, L.: Pyramid vision transformer: A versatile backbone for dense prediction without convolutions. In: Proceedings of the IEEE/CVF International Conference on Computer Vision (2021) [4](#), [10](#), [11](#)
87. Wang, W., Xie, E., Li, X., Fan, D.P., Song, K., Liang, D., Lu, T., Luo, P., Shao, L.: Pvtv2: Improved baselines with pyramid vision transformer. Computational Visual Media (2022) [7](#)

88. Wang, Z., Ma, C.: Semi-Mamba-UNet: Pixel-Level Contrastive Cross-Supervised Visual Mamba-based UNet for Semi-Supervised Medical Image Segmentation (2024) [4](#)
89. Wang, Z., Zheng, J.Q., Zhang, Y., Cui, G., Li, L.: Mamba-UNet: UNet-Like Pure Visual Mamba for Medical Image Segmentation (2024) [4](#)
90. Williams, R.L., Lawrence, D.A., et al.: Linear state-space control systems. John Wiley & Sons (2007) [2](#), [5](#)
91. Woo, S., Debnath, S., Hu, R., Chen, X., Liu, Z., Kweon, I.S., Xie, S.: ConvNeXt V2: Co-designing and Scaling ConvNets with Masked Autoencoders. In: CVPR (2023) [3](#)
92. Wu, H., Xiao, B., Codella, N., Liu, M., Dai, X., Yuan, L., Zhang, L.: Cvt: Introducing convolutions to vision transformers. In: Proceedings of the IEEE/CVF International Conference on Computer Vision (2021) [4](#)
93. Wu, Z., Shen, C., Van Den Hengel, A.: Wider or deeper: Revisiting the resnet model for visual recognition. *Pattern Recognition* **90**, 119–133 (2019) [13](#)
94. Xiao, T., Liu, Y., Zhou, B., Jiang, Y., Sun, J.: Unified perceptual parsing for scene understanding. In: Proceedings of the European conference on computer vision. pp. 418–434 (2018) [1](#), [12](#)
95. Xie, S., Girshick, R., Dollár, P., Tu, Z., He, K.: Aggregated Residual Transformations for Deep Neural Networks. In: CVPR (2016) [1](#), [3](#)
96. Xie, S., Girshick, R., Dollár, P., Tu, Z., He, K.: Aggregated residual transformations for deep neural networks. In: Proceedings of the IEEE conference on computer vision and pattern recognition. pp. 1492–1500 (2017) [10](#), [11](#)
97. Xu, W., Xu, Y., Chang, T., Tu, Z.: Co-scale conv-attentional image transformers. In: Proceedings of the IEEE/CVF International Conference on Computer Vision. pp. 9981–9990 (2021) [4](#)
98. Xu, Y., Zhang, Q., Zhang, J., Tao, D.: Vitae: Vision transformer advanced by exploring intrinsic inductive bias. *Advances in Neural Information Processing Systems* **34**, 28522–28535 (2021) [4](#)
99. Xue, F., Shi, Z., Wei, F., Lou, Y., Liu, Y., You, Y.: Go wider instead of deeper. In: Proceedings of the AAAI Conference on Artificial Intelligence. vol. 36, pp. 8779–8787 (2022) [13](#)
100. Yang, C., Xu, J., Mello, S.D., Crowley, E.J., Wang, X.: GPViT: A High Resolution Non-Hierarchical Vision Transformer with Group Propagation [2](#), [4](#), [5](#), [9](#), [10](#), [12](#)
101. Yang, J., Li, C., Zhang, P., Dai, X., Xiao, B., Yuan, L., Gao, J.: Focal self-attention for local-global interactions in vision transformers. In: NeurIPS (2021) [10](#), [11](#), [12](#)
102. Yun, S., Han, D., Oh, S.J., Chun, S., Choe, J., Yoo, Y.: Cutmix: Regularization strategy to train strong classifiers with localizable features. In: Proceedings of the IEEE/CVF international conference on computer vision. pp. 6023–6032 (2019) [10](#)
103. Zhai, X., Kolesnikov, A., Houlsby, N., Beyer, L.: Scaling Vision Transformers. In: CVPR (2022) [5](#)
104. Zhang, H., Cisse, M., Dauphin, Y.N., Lopez-Paz, D.: mixup: Beyond empirical risk minimization. *arXiv preprint arXiv:1710.09412* (2017) [10](#)
105. Zhang, P., Dai, X., Yang, J., Xiao, B., Yuan, L., Zhang, L., Gao, J.: Multi-Scale Vision Longformer: A New Vision Transformer for High-Resolution Image Encoding. *arXiv.org* (Mar 2021) [11](#)
106. Zhong, Z., Zheng, L., Kang, G., Li, S., Yang, Y.: Random erasing data augmentation. In: Proceedings of the AAAI conference on artificial intelligence (2020) [10](#)

107. Zhou, B., Zhao, H., Puig, X., Fidler, S., Barriuso, A., Torralba, A.: Scene parsing through ade20k dataset. In: Proceedings of the IEEE Conference on Computer Vision and Pattern Recognition (July 2017) [1](#), [4](#)
108. Zhu, L., Liao, B., Zhang, Q., Wang, X., Liu, W., Wang, X.: Vision mamba: Efficient visual representation learning with bidirectional state space model. arXiv preprint arXiv:2401.09417 (2024) [2](#), [3](#), [4](#), [6](#), [7](#), [8](#), [10](#), [12](#), [13](#)